Acta Crystallographica Section B
Structural Science
ISSN 0108-7681

Chiral determination: direct interpretation of convergent-beam electron diffraction patterns using the series expansion of Cowley and Moodie

Andrew W. S. Johnson

Centre for Microscopy and School of Physics, University of Western Australia, Crawley, 6009, Australia

Correspondence e-mail: bill@physics.uwa.edu.au

Received 26 April 2007
Accepted 11 June 2007

Given a small number of structure factors of a known chiral structure of unknown hand, it is shown that the hand can be determined from the sign of the contrast difference of two reflections in a suitably oriented convergent-beam electron diffraction (CBED) pattern. A simple formula for this difference, which takes into account all the significant second-order scattering, is derived using the series expansion of Cowley and Moodie for *n*-beam diffraction. The reason for the success of a three-beam interpretation is investigated. The method is applied to patterns from thin crystals in which a mirror projection symmetry can be found and its validity is demonstrated by agreement with experiment using samples of known hand. The advantages of recording patterns near major zone axes are discussed as well as some other experimental aspects of chiral determination using CBED.

1. Introduction

It has been known for a few decades that the hand of chiral structures can be determined from convergent-beam electron diffraction (CBED) experiments (Goodman & Secomb, 1977; Goodman & Johnson, 1977; Tanaka *et al.*, 1985; Johnson & Preston, 1994). This ability is due to multiple scattering within the crystal leading to an exit wave on which the relative phases (as well as the amplitudes) of the Fourier coefficients of the crystal potential have a significant influence. Early determinations used data from two patterns at differing orientations, making for a more difficult experiment. A single pattern is preferable but, if taken at an exact zone axis for example, requires a full multislice calculation to determine hand.[1] It is attractive to use a pattern which can be interpreted using only a few structure factors in a simple calculation, but such an aim needs to be carefully validated before use.

The use of a thin crystal is an advantage since it simplifies the calculation and allows the use of a projected ZOLZ (zero-order Laue zone) mirror plane for orientating the crystal, the influence of HOLZ (high-order Laue zone) reflections on the ZOLZ symmetry being minimal for thin crystals. In this respect the previous work on the enantiomorphisim using a single CBED pattern of low quartz (Goodman & Johnson, 1977) was made more difficult by the use of a thick crystal. In the case of low quartz, multiple scattering within the ZOLZ is essential for the identification of mirror planes and hence the indexing (Goodman & Secomb, 1977), and it will be seen later that a modification of the analytical method to be described may possibly be applied to such cases.

[1] The comment by Johnson & Preston (1994) in referring to the chiral character of a 111 axis pattern of $Bi_{12}GeO_{20}$ (mistakenly referred to as $Bi_{12}GeO_{24}$) that hand cannot be determined from such patterns is incorrect.

Table 1
Zone axes of patterns with projected mirror lines in their ZOLZ, polar axes and non-polar directions for point groups which support enantiomorphisim.

All directions normal to an even-fold rotation axis are non-polar. The symmetry-equivalent sets of directions are placed between semicolons in the fourth column. Hexagonal indices are used for the rhombohedral groups.

Point group	Zone axes with a mirror line or lines	Polar (symmetry) axes	Non-polar directions
432	⟨001⟩ ⟨110⟩ ⟨111⟩	None	[0*uw*] [*u*0*w*] [*uv*0]; [*uuw*] [*uvv*] [*uvu*]; [*u*−*uw*] [*uv*−*v*] [−*uvu*]
23	⟨001⟩ ⟨110⟩	Four threefold	[0*uw*] [*u*0*w*] [*uv*0]
622	⟨001⟩ ⟨100⟩ ⟨210⟩	None	[*u*2*uw*] [−2*u*−*uw*] [*u*−*uw*] [*uuw*] [−*u*0*w*] [0−*vw*]
6	None	[001]	[*uv*0]
3	None	[001]	None
312	⟨001⟩ ⟨100⟩	[1$\bar{1}$0] [120] [$\bar{2}\bar{1}$0]	[*uuw*] [−*u*0*w*] [0−*vw*]
321	⟨001⟩ ⟨210⟩	[100] [010] [$\bar{1}\bar{1}$0]	[*u*2*uw*] [$\bar{2}$*u*−*uw*] [*u*−*uw*]
422	⟨001⟩ ⟨100⟩ ⟨110⟩	None	[*uv*0]; [0*vw*] [*u*0*w*]; [*uuw*] [*u*−*uw*]
4	None	[001]	[*uv*0]
222	⟨100⟩ ⟨010⟩ ⟨001⟩	None	[0*uv*]; [*u*0*w*]; [*uv*0]
2	⟨001⟩ ⟨100⟩ unique axis *b*	[010]	[*u*0*w*]

The present paper is an extension of work on a simple experimental method of hand determination from a single CBED pattern reported by Johnson & Preston (1994). In that paper, the interpretation was made using either full *n*-beam or three-beam calculations. However, a full *n*-beam calculation is tedious and a three-beam calculation over-emphasizes the coupling between three beams, omitting the possible influence on the result of other beams visible in the diffraction pattern. Here, provided the crystal is sufficiently thin, the calculation is greatly simplified by the use of a simple formula derived by summing the first- and second-order scattering processes of the series expansion for *n*-beam diffraction of Cowley and Moodie (Cowley & Moodie, 1962; Moodie, 1972). Further, the influence of other beams in the diffraction pattern is investigated.

An important aspect of the method of Johnson & Preston (1994) is that the crystal is orientated such that a twofold axis, either rotor or screw, is perpendicular to the incident electron beam. This situation results in a mirror line, or lines, of intensity symmetry in the ZOLZ at a zone axis. The crystal is then tilted, maintaining a mirror line of symmetry in the ZOLZ until a pair of chirally sensitive reflections is observed in the first-order Laue zone that break the mirror. Such reflections are known in X-ray crystallography as equivalents or Bijvoet pairs. It is important to realise that not all such pairs are equally sensitive to the chiral nature of the crystal when excited in a multiple beam experiment. This experimental technique of rotation of the crystal about an axis normal to the mirror line automatically exposes those pairs of reflections that are sensitive to hand. In addition, a tilted pattern has the advantage of simplifying the diffraction conditions, permitting the deduction of a simple formula such as that derived in §4 of this paper.

There is little in the literature on the selection of zone axes suitable for chiral determination by CBED. From a consideration of previous work on the subject it is clear that the type of analysis and the ease of the experiment depend on the choice of zone axis. This arises because some projections result in polar twofold axes and when these are present, dynamic interaction within the ZOLZ may reduce the observed projection symmetry from that expected. Therefore, it is useful to consider the projected symmetry and it is discussed in §2 of this paper.

Some observations on the use of minor zone axes and a paper on CBED chiral determination (Inui *et al.*, 2003) are made in §11.

2. Experimental

In recording a CBED pattern suitable for chiral determination, the facility offered by the presence of a ZOLZ mirror line in maintaining the correct orientation whilst tilting should not be underestimated. In choosing a zone axis for a chiral determination, both experimental and analytical factors should be considered. Experimentally, both the ease of recognizing the zone symmetry and in subsequently tilting to the required orientation are important, and analytically, the determination of a unique index and the degree of computation required. These issues become relevant when dealing with large unit-cell structures.

Before proceeding with a brief description of the experiment, some remarks on indexing should be made. The method depends on the zone axis used. If the projection contains polar axes, a dynamic calculation is required to distinguish the sense of the axes and hence the correct index. This is possible in CBED from a thin crystal as the internal ZOLZ interactions are dynamic (Friedel's Law does not hold). Projections with plane-group symmetry *pm*, *pg*, *p*31*m* or *p*3*m*1 will have a polar direction. When the projection has no polar axis, either the measurement of the axial ratio or the calculation of structure factors, in the case of a square lattice, will determine a unique index.

To aid in understanding the above, it is useful to consider the following examples. MnSi has the cubic space group 198, $P2_13$. If the 001 zone is used, *p*2*gg* plane-group symmetry is found, all ZOLZ structure factors are real and two mirror lines

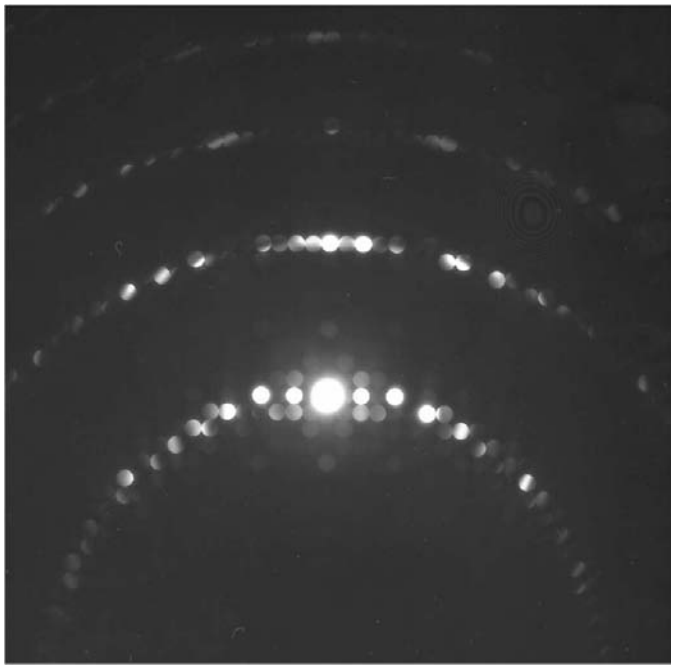

Figure 1
A typical orientation for hand determination. The mirror symmetry in the ZOLZ is clearly seen, broken in the FOLZ. Aligned with the horizontal direction of this figure is a screw axis causing odd-order extinctions in the ZOLZ. The space group is $P4_12_12$ or its enantiomorph and the pattern is taken near the fourfold axis

will be seen. However, the 110 zone (symmetry *p*1*g*1) was chosen by Tanaka *et al.* (1985) and the ZOLZ is consequently asymmetric (polar) and a dynamic calculation was used to determine its sense. Another example, $Bi_{12}GeO_{20}$[2] (Johnson & Preston, 1994) with the cubic space group 197, *I*23, has a projected symmetry of *p*2*mm* in the 001 zone. As the diffraction pattern is square but the symmetry only 2*mm*, calculation of the ZOLZ structure factors will be needed to distinguish between the *a** and *b** axes before a unique index can be established.[3]

The enantiomorphic point groups 3, 4 and 6 require special consideration as they do not have mirror lines in any projection. The present treatment does not cover these groups which present the experimental difficulties discussed in §9. When a twofold axis is present a mirror will result. An example is low quartz (trigonal, space group 152, $P3_121$). When viewed down 001, the zero-order zone is polar with projection symmetry *p*31*m*. Dynamic interactions within this zone result in a diffraction pattern with threefold symmetry and this allows the sense of the mirror line in relation to the structure to be determined, as shown by Goodman & Secomb (1977). The method of Goodman & Secomb could be adapted to thin crystals, with smaller tilts than they used and applying expression (6) in a modified form appropriate for a ZOLZ having complex structure factors as discussed in §9.

[2] The use of the term BGO is confusing since it is being applied to both $Bi_{12}GeO_{20}$ and $Bi_4Ge_3O_{12}$.
[3] This point was not explained in the paper by Johnson & Preston (1994).

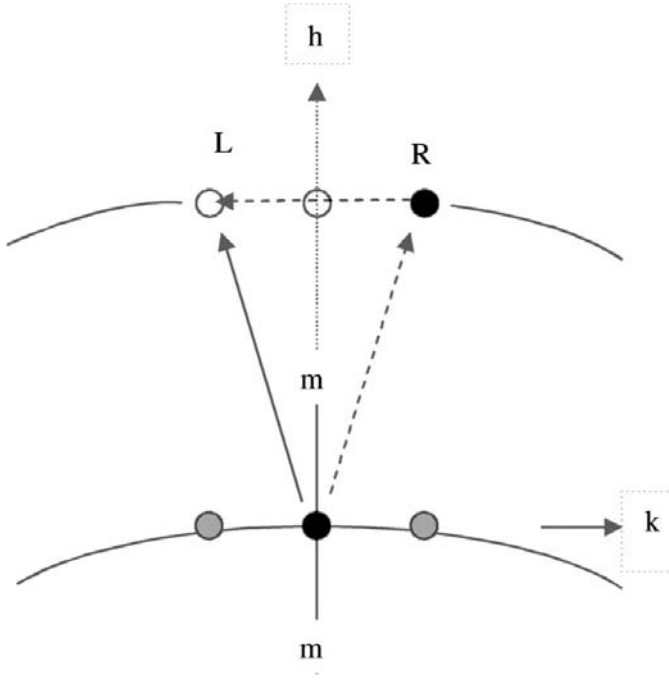

Figure 2
Two possible one- and two-segment paths to the beam **L**.

To assist in setting up an experiment, the zone axes with projected mirror lines for the point groups supporting enantiomorphism are given in Table 1. In addition, the right-most two columns are selected entries from Table 10.5.2 of the *International Tables for Crystallography* (1992) for the identification of polar mirror lines and directions, and thus the diffraction symmetry of the zero-order Laue zone under conditions of multiple scattering when the crystal is thin.

2.1. Example

A CBED pattern from $Ho_2Ge_2O_7$ at an orientation[4] suitable for hand determination is shown in Fig. 1. This orientation is near, *but not at*, a major zone axis, the latter being easy to obtain and index. After recognizing a mirror line, or lines, of projected symmetry in the ZOLZ, refinement of the orientation was made by rotating the crystal away from the zone axis about an axis perpendicular to the mirror line (in this case a twofold screw axis was used) until a large intensity difference was noted between equivalent reflections in the first-order zone. The equivalent reflections in the FOLZ of Fig. 1 are those labelled L and R in Fig. 2, which is a simplified diagrammatic representation of Fig. 1.

Indexing a diffraction pattern that shows two or more Laue zones without ambiguity depends on the space group of the crystal. As discussed earlier, the symmetry of the 'special projection' must be considered and the sense of the mirror line, if polar, taken account of. As the curvature of the Ewald sphere is always towards the crystal, choosing a right-handed reciprocal set of axes *h*, *k* and *l* with the *l* axis in the beam direction results in the first-order zone index −1. This

[4] In this case the 001 zone which has *p*4*gm* ZOLZ symmetry.

indexing is consistent with the requirements in the note published by Spence *et al.* (1994) on the minimum number of beams (four) required to distinguish enantiomorphism.[5]

The crystal giving the pattern of Fig. 1 was used to record further patterns at other rotations so that a more stringent test of the formula derived later in this paper could be made. This test is discussed in §7.

3. Background

It was shown previously (Johnson & Preston, 1994), by comparison of experiment with a full *n*-beam calculation, that a three-beam interpretation of the intensity difference between a pair of equivalent reflections in the first-order Laue zone could be sufficient to determine hand, provided the crystal was thin and the experimental conditions were chosen appropriately. In the examples given, $Bi_{12}GeO_{20}$ and $Ho_2Ge_2O_7$, the sign of the contrast difference showed no tendency to reverse at thicknesses of 30 nm or more, independent of the number of beams used in the dynamical calculation. This result was repeated in the three-beam calculation. However, as stated previously, a three-beam analysis over-emphasizes the coupling between the beams and omits the possible influence on the result of other beams visible in the diffraction pattern. These factors led to a re-examination of the diffraction situation using the series expansion of the *n*-beam diffraction of Cowley and Moodie. This showed that it is possible to derive an approximation, other than the three-beam, which takes into account the influence of more of the beams at the expense of limiting the extent of the interaction. This approximation only includes the coupling between the beams at or near zero excitation error (those that are visible in the diffraction pattern) and gives a simple formula to determine the hand. It is the main subject of the present paper.

4. Theory

Our aim is to calculate the relative intensity of the equivalent reflections, L and R in Fig. 2, using only the first- and second-order interactions in the series expansion by Cowley and Moodie of *n*-beam diffraction. In the expansion, the amplitude $\mathbf{U}$[6] of the diffracted beam $\mathbf{h}$ is shown to be the sum of products of two functions

$$\mathbf{U}(\mathbf{h}) = \sum_{n=1} \mathbf{V}_n(\mathbf{h})\mathbf{Z}_n(\mathbf{h}), \tag{1}$$

where $\mathbf{V}$ is a function dependent on the Fourier coefficients of the potential, $\mathbf{Z}$ is dependent only on the geometry of the experiment and n is the order of interaction. It can be shown for reflections close to the Ewald sphere that $\mathbf{Z}$ can be approximated by $1/n!$ (Cowley & Moodie, 1962[7]). In this instance (1) is the thin-phase grating approximation expressed in reciprocal space. Since our purpose here is simply to determine which of two equivalent diffracted beams is of greater intensity and the experiment is designed to maximize the difference, this approximation is sufficient.

The function $\mathbf{V}$ is a product of n terms of the form $i\sigma HV(h_j)$, where σ is the scattering coefficient, H is the thickness and $V(h_j)$ is the h_j Fourier coefficient of the potential for one unit cell. The interpretation of this product can be understood when it is viewed as a multiple scattering diagram, as described by Gjønnes & Moodie (1965). This view represents the total amplitude $\mathbf{U}(\mathbf{h})$ of a diffracted beam $\mathbf{h}$ as the sum over all possible paths in the diffraction pattern, each segment of a path, j, having the complex scattering probability of $i\sigma H V(h_j)$. For a thin crystal, owing to the small factor σH, paths of one or two segments, $n = 1$ or 2, will dominate the sum, as the influence of third- and higher-order terms may be neglected.

Of the sets of possible equivalent reflections that may be excited in the first-order Laue zone, a pair with a large difference in intensity is chosen experimentally. This pair is labeled L and R and we now calculate their intensity difference. Contributions to the amplitude, $\mathbf{U_l}$, of the beam L for paths of one and two segments can be seen by inspection of Fig. 2 where the one segment path is represented by the full line vector and a typical two segment path is dotted. In the following, the Fourier coefficients of interzone vectors are represented using upper-case symbols and intrazone by lower-case.

Following Cowley & Moodie, the amplitude of beam L is

$$\begin{aligned} U_{\rm L} = {} & i\sigma H V_{\rm L} \exp(i\Phi_{\rm L}) + \frac{(i\sigma H)^2}{2!} 2v_c V_{\rm R} \exp(i\Phi_{\rm R}) \\ & + \frac{(i\sigma H)^2}{2!} \sum_{i=1}^{p} v_{\rm o} F_{\rm L} + \text{terms in } (i\sigma H)^3/3! \text{ and} \\ & \text{higher powers}, \end{aligned} \tag{2}$$

where $V_{\rm L}$, $\Phi_{\rm L}$, $V_{\rm R}$ and $\Phi_{\rm R}$ are the amplitudes and phases of the equivalent reflections L and R, respectively, and $v_{\rm c}$ is the coupling term between them. The first term in (2) is the one segment path, the next term is the sum of those two segment paths which involve an equivalent reflection coupled by $v_{\rm c}$ (Fig. 3*a*) and the third term is the sum over the remaining p two-segment paths involving a zero- or first-zone vector, $\mathbf{v_o}$, and an inter-zone vector $\mathbf{F_L}$. A selection of these latter paths are shown in Figs. 3(*b*)–(*f*).

Calculating the intensity of the beam L from (2) yields, after some simplification, neglecting terms of order $(i\,\sigma\,H)^3/3!$ and higher, and replacing $V_{\rm R}$ by $V_{\rm L}$

$$\begin{aligned} I_{\rm L} = {} & V_{\rm L}^2 + 2\sigma H v_{\rm c} V_{\rm L}^2 \sin(\Phi_{\rm L} - \Phi_{\rm R}) - \frac{i\sigma H}{2!} \sum \{v_{\rm L}^* V_{\rm L} F_{\rm L}^* \\ & - v_{\rm L} V_{\rm L}^* F_{\rm L}\}, \end{aligned} \tag{3}$$

[5] In the paper by Johnson & Preston (1994) there is a note added in the proof in which an apparent contradiction was mentioned. The contradiction, simply resolved, was that, although four non-coplanar beams are required for indexing, subsequently only three beams are required for hand determination. Provided polar effects are considered, an electron diffraction pattern showing two or more zones can always be uniquely indexed due to the fact that the Ewald sphere curves toward the crystal.

[6] Bold case is used for functions and vectors.

[7] The factor 2π in this original derivation drops out of $\mathbf{Z}$ with a symmetric definition of the Fourier transform.

where a common multiplier σH in (2) has been omitted.

The right hand term of (3)

$$\frac{-i\sigma H}{2!}\sum_{i}^{p}\{v_{\rm L}^{*}V_{\rm L}F_{\rm L}^{*}-v_{\rm L}V_{\rm L}^{*}F_{\rm L}\} \qquad (4)$$

contains the significant two-term processes, each labelled i and p in number, which end on L but *do not* involve the coupling term $v_{\rm c}$. The intra- and inter-zone coefficients are $v_{\rm L}$ and $F_{\rm L}$, respectively.

After simplifying (4) and noting that $v_{i,\rm L}$ is real[8] when a mirror line exists in the ZOLZ, (3) can be written

$$I_{\rm L}=V^{2}+2\sigma Hv_{\rm c}V^{2}\sin(\Phi_{\rm L}-\Phi_{\rm R})+\sigma HV\sum_{i}^{p}|v_{i,\rm L}||F_{i,\rm L}|\sin(\Phi_{\rm L}-\theta_{i,\rm L}), \qquad (5)$$

where $\theta_{i,\rm L}$ is the phase angle of the product $v_{i,\rm L}\,F_{i,\rm L}$ and the suffix on V is no longer necessary as the amplitudes of $V_{\rm L}$ and $V_{\rm R}$ are equal.

The intensity of beam R, found by interchanging the subscripts L and R in (5), is subtracted from (5) to give

$$\Delta I_{\rm L-R}=4\sigma Hv_{\rm c}V^{2}\sin(\Phi_{\rm L}-\Phi_{\rm R})+\sigma HV\sum_{i}^{p}|v_{i,\rm L}||F_{i,\rm L}|\sin(\Phi_{\rm L}-\theta_{i,\rm L})-\sigma HV\sum_{j}^{p}|v_{j,\rm R}||F_{j,\rm R}|\sin(\Phi_{\rm R}-\theta_{j,\rm R}), \qquad (6)$$

where the introduction of subscript j denotes that the two summations are independent.

We may simplify (6) by introducing the phase and amplitude relationships between the left and right equivalent structure factors that result from using the ZOLZ mirror line for experimental alignment. For the present consider just the relationships for space groups $P2$ and $P2_1$ to cover those point groups with a projected mirror symmetry that support enantiomorphism.[9] With the pattern indexed as shown in Fig. 4, the relationships of use, taken from *International Tables for X-ray Crystallography* (1952), are $|F(hkl)|=|F(h\bar{k}l)|$, $\alpha(hkl)=-\alpha(h\bar{k}l)$ for $P2$ and for $P2_1$ when k is even and, additionally for $P2_1$, when k is odd, $|F(hkl)|=|F(h\bar{k}l)|$, $\alpha(hkl)=\pi-\alpha(h\bar{k}l)$.

For simplicity, consider $P2$. In this case $\Phi_{\rm L}=-\Phi_{\rm R}$, v is real due to the mirror line, and $\theta_{i,\rm L}=-\theta_{i,\rm R}$. In applying these to the simplification of (6), it is helpful to use the scattering diagrams depicted for a limited diffraction pattern in Fig. 4. Two segment paths can be chosen, reflected across the ZOLZ mirror line, to pair left and right terms that are equivalent. The possible paths are depicted in Fig. 3 for only the beam L. The paths to the beam R are those for L mirrored across the dashed line. Hence, the paths shown in Fig. 3(*a*) together with those in the mirror of Fig. 3(*a*) (those to R) are all contained in the first term of (6). The remaining diagrams in Fig. 3 are the paths contained in the second term of (6) with the mirror of these in the third term of (6). For Figs. 3(*b*) and (*c*) both the amplitudes and phases of $v_{\rm L}$ and $F_{\rm L}$ are equal to $v_{\rm R}$ and $F_{\rm R}$, respectively, hence when choosing appropriate terms from the summations in (6), they are cancelled.

For Figs. 3(*d*), (*e*) and (*f*) both the amplitude and phase of $v_{i,\rm L}$ is equal to $v_{j,\rm R}$ and $F_{j,\rm R}$ is the conjugate of $F_{i,\rm L}$. Hence we may write (6) as

$$\Delta I_{\rm L-R}=4\sigma Hv_{\rm c}V^{2}\sin(2\Phi_{\rm L})+2\sigma HV\left\{\sum_{i}^{<p}|v_{i,\rm L}||F_{i,\rm L}|\sin(\Phi_{\rm L}-\theta_{i,\rm L})\right\}, \qquad (7)$$

where the summation is now only over the paths (*d*), (*e*) and (*f*) in Fig. 3, as indicated by the < symbol in the upper limit. By making use of the fact that V is approximately $|F_{i,\rm L}|$ and the

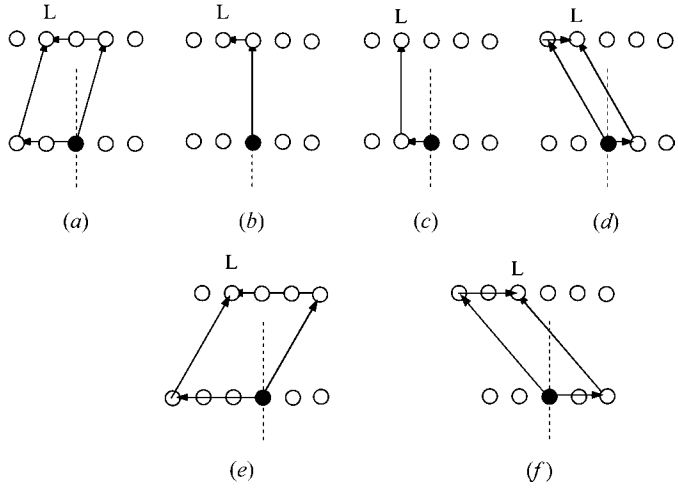

Figure 3
Scattering diagrams for two term paths to beam L in a typical pattern. The dashed line is the ZOLZ mirror line.

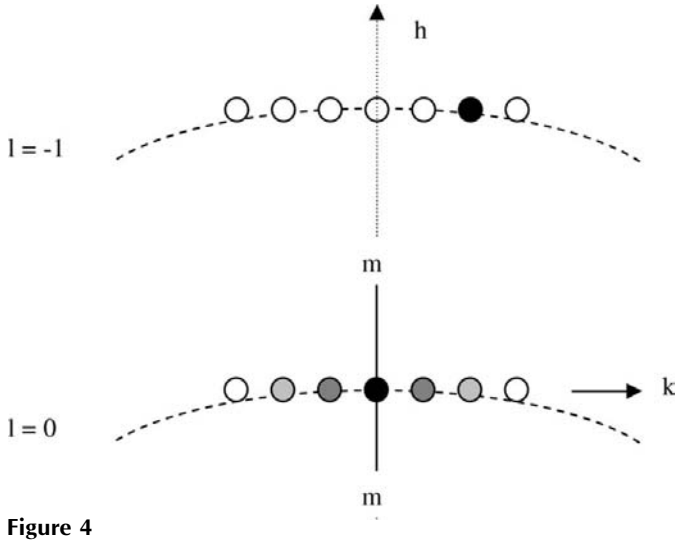

Figure 4
The definition of indexing for $P2$ and $P2_1$.

[8] The case of $v_{i,\rm L}$ complex is discussed later in this paper.
[9] Trigonal point groups are best treated separately, the mirror line being polar, as described elsewhere in this paper.

mean intensity of L and R is $(\sigma HV)^2$, (7) may be recast in terms of contrast as

$$C_{\mathrm{L-R}} \simeq 2\sigma H\left[2v_{\mathrm{c}}\sin(\Phi_{\mathrm{L}}-\Phi_{\mathrm{R}})+\sum_{i}^{<p}|v_{i,\mathrm{L}}|\sin(\Phi_{\mathrm{L}}-\theta_{i,\mathrm{L}})\right]. \tag{8}$$

Knowing the phases and amplitudes of the Fourier coefficients in the diffraction pattern from a structure factor calculation, (8) can be readily evaluated and the hand determined.

5. Extension to 2_1

No terms for k odd can exist in the scattering diagrams in Fig. 3. There is hence no coupling with relative phases of $\alpha(hkl) = \pi - \alpha(h\bar{k}l)$ and the foregoing analysis for $P2$ is sufficient. When paths in the ZOLZ with h non-zero are considered a different circumstance exists for a glide mirror line. This is discussed later.

6. Discussion

It is found that the sign of the intensity difference calculated using only the first term of (7) gives the same hand as both the three beam and full multislice calculations for the examples given in the earlier work of Johnson & Preston (1994). These are for tilted patterns, such as Fig. 1, some showing many more ZOLZ reflections than that considered in Fig. 3. From this result, it appears that paths *via* these additional ZOLZ beams, those contained in the remaining terms in the summation of (7), have little magnitude relative to the first term and have only a small influence for the type of orientation considered. To avoid a false determination it is important to understand the conditions under which this occurs.

A minimum in the summation of (7) clearly depends on the values of phase angles $\theta_{i,\mathrm{L}}$ relative to Φ_{L}, as well as the amplitudes and phases of $v_{i,\mathrm{L}}$. However, these parameters are structure dependent and at least the phase angles should be calculated for the case being considered.

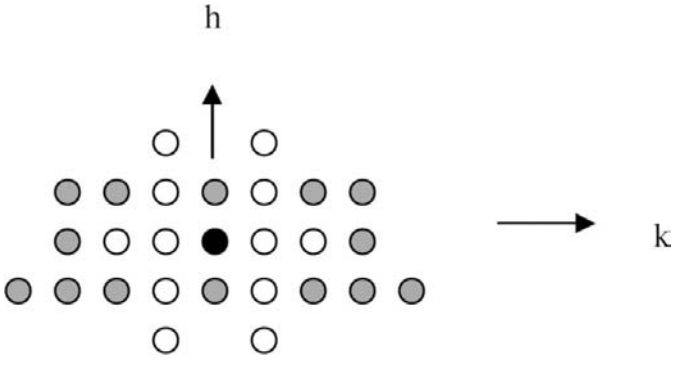

Figure 5
Typical ZOLZ reflections involved in two term paths to beams L and R. See the text for an explanation of the shading.

There are further aspects of the above approximation that are of interest. One is to extend our consideration to ZOLZ reflections of the form $hk0$, another is to consider covering point groups 321 and 312, and a third is to derive the above theory in a form suitable for zone-axis patterns such as those promoted by Inui *et al.* (2003).

6.1. Extension to ZOLZ reflections when h is non-zero

When Fig. 3 is extended to include ZOLZ reflections for h non-zero, it is readily shown that for v_{hk0} real, all the paths to L and R *via* the ZOLZ reflections, shown as open circles in Fig. 5, are either accounted for by the first term in (6) or cancel between the summation terms in (6). The grey circles represent the remaining beams whose influence requires assessing.

It is convenient to return to the form of the summation term given in (4) rather than that of (6). For brevity, it is assumed that that the coupling term is 020.

We then have

$$\frac{-i\sigma H}{2!}\left[\sum_{i}^{p}{}_{i}\{v_{\mathrm{L}}^{*}V_{\mathrm{L}}F_{\mathrm{L}}^{*}-v_{\mathrm{L}}V_{\mathrm{L}}^{*}F_{\mathrm{L}}\}\right.$$
$$\left.-\sum_{j}^{p}{}_{j}\{v_{\mathrm{R}}^{*}V_{\mathrm{R}}F_{\mathrm{R}}^{*}-v_{\mathrm{R}}V_{\mathrm{R}}^{*}F_{\mathrm{R}}\}\right]. \tag{9}$$

Picking out only the term i in this expression for the path shown in Fig. 6 to L and the equivalent term, j, for the path to R, and using, for simplicity, $v = v_{\mathrm{L}} = v_{\mathrm{R}}$ (equal to a real number), as well as using the Bijvoet relations between V_{L} and V_{R} and between F_{L} and F_{R}, we can write for these two terms, $(-i\sigma H/2!)2v[\{V_{\mathrm{L}}F_{\mathrm{L}}^{*}-V_{\mathrm{L}}^{*}F_{\mathrm{L}}\}]$. Then (9) simplifies to $\sigma Hv[\Im\{V_{\mathrm{L}}F_{\mathrm{L}}\}]$, where $\Im$ indicates the imaginary part.

Substituting

$$V_{\mathrm{L}} = \sum_{\mathrm{atom}} f_{\mathrm{atom}}[A_{\mathrm{atom},V} + iB_{\mathrm{atom},V}] \text{ and}$$
$$F_{\mathrm{L}} = \sum_{\mathrm{atom}} f_{\mathrm{atom}}[A_{\mathrm{atom},F} + iB_{\mathrm{atom},F}]$$
$$\text{for } \Im\{V_{\mathrm{L}}F_{\mathrm{L}}\} \text{ gives for each atom, } \sigma Hv[\{B_{v}A_{F} - A_{v}B_{F}\}]. \tag{10}$$

Considering further simplification, it is easier to deal with the structure-factor expression for the space group $P222$, in which all $hk0$ structure factors are real and, besides being

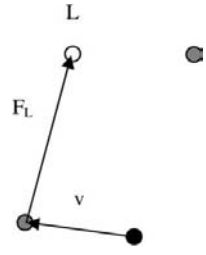

Figure 6
A typical path to L considered in $P222$ to estimate the magnitude of the summation term of equation (7).

Table 2
Comparison of experimental observations with calculation of the first term of (8) for $P4_12_12$ and $P4_32_12$.

hkl for the FOLZ pair	7 −2 −1 7 2 −1	9 −2 −1 9 2 −1	10 −2 −1 10 2 −1	11 −1 −1 11 1 −1	11 −2 −1 11 2 −1	17 −2 −1 17 2 −1 zone axis
(*a*) $P4_12_12$						
$\|V\|$ and phase for $P4_12_12$	1.0, 311^0 139^0	0.57, 105^0 345^0	0.34, 42^0 228^0	0.32, 47^0 223^0	0.3, 127^0 323^0	0.18, 121^0 329^0
$v_c \sin(\Phi_L - \Phi_R)$	−0.6	−4.0	−0.4	0.05	−1.2	−2.2
Δ_{L-R} experiment	−	−−−	−	++	−	−−
(*b*) $P4_32_12$						
$\|V\|$ and phase for $P4_32_12$	0.6, 46^0 224^0	0.73, 44^0 266^0	0.34, 342^0 108^0	0.37, 82^0 8^0	0.18, 193^0 77^0	0.05, 76^0 194^0
$v_c \sin(\Phi_L - \Phi_R)$	0.16	−3.1	3.7	0.73	−4.1	4.0
Δ_{L-R} experiment	−	−−−	−	++	−	−−

mirrored across the line $h = 0$, are also across $k = 0$. The general structure-factor expressions in this group are

$$|F(hkl)| = |F(h\bar{k}l)|,$$

and

$$\alpha(hkl) = \alpha(h\bar{k}l),$$

where we can permute h, k and l and the structure factor components for each atom are

$$A = 4\cos(2\pi hx)\cos(2\pi ky)\cos(2\pi lz)$$

and

$$B = -4\sin(2\pi hx)\sin(2\pi ky)\sin(2\pi lz).$$

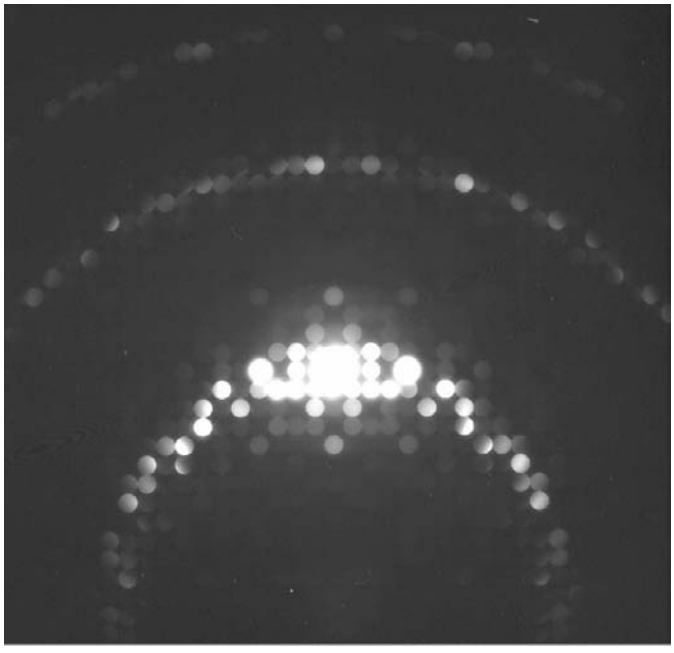

Figure 7
The pattern headed '11 −1 −1, 11 1 −1' in Table 2. Comparison of the FOLZ pair 11 −1 −1/11 1 −1 gives an answer for the hand opposite that found for the other experimental data. See text for details.

To make the result more independent of structure, the scattering from each atom is considered rather than the structure factor. We have $F_{atom} = f_{atom}[A + iB]$, where f_{atom} is the atomic scattering factor and now V and F refer to an atom. For convenience, the expressions for A and B are shortened to ccc and −sss and note that both V and F have approximately the same scattering vector as well as the terms hx, ky and lz. Then (10) becomes

$$\sigma Hv[-\text{sss.ccc} + \text{ccc.sss}]$$

which is approximately zero when averaging over all the atoms in the unit cell is taken account of.

From this it can be seen that the collective effect of the remaining paths, *via* the ZOLZ (grey circles in Fig. 5), on the intensity difference is small, allowing the first term of (7) to dominate.

If the plane-group symmetry of the ZOLZ is *p*4*gm*, as in the example below using $Ho_2Ge_2O_7$, the *hk*0 reflections mirror across the line $k = 0$ when $h + k$ is even, but are opposite when $h + k$ is odd. Hence, (7) is valid for all paths when $h = 0$, but not necessarily otherwise.

7. Results

7.1. $Ho_2Ge_2O_7$

Data taken from a series of different tilts are shown in Table 2. Calculations of structure factors were made for both enantiomorphic space groups $P4_12_12$ and $P4_32_12$ using the *Xtal* crystallographic program[10] and data from Smolin (1970). The values of $v_c \sin(\Phi_L - \Phi_R)$ from (8) are shown along with the relevant structure factors. For v_c, values of −0.76 and −4.6 V were used for the 020 and 040 structure factors, respectively.

Apart from the case of the 11 − 1 −1 and 11 1 −1 pair, the agreement between the calculated and experimental rows in each section of Table 2 is good for $P4_12_12$, but poor for $P4_32_12$. All experimental data has been included so patterns that show little contrast are also shown. These would not be expected to give a definitive result in determining hand.

The 11 −1 − 1 and 11 1 −1 pair give an opposing result to the remainder of the data. The pattern is reproduced in Fig. 7. It is clear that the ZOLZ intensities are much greater than those of the HOLZ. Further, the strength of the coupling term 020, used to determine the hand, is much less than that of 040 clearly seen in the ZOLZ and in agreement with the calculated values (−4.6 and −0.8 V, respectively) of these structure factors. Thus, paths *via* the 0 4 0 + 11 −5 −1 and 0 −4 0 + 11 3 −1 are considerably stronger than the 0 2 0 + 11 −1 −1 and 0−2 0 + 11 1 −1 pairs, assumed to be dominant in the derivation of expression (8) used to determine the hand. Also, there are many *h* non-zero paths in the ZOLZ where, due to

[10] Version 3.7 available *via* http://xtal.sourceforge.net.

the glide mirrors resulting from the projection of two 2_1 screw axes (plane-group symmetry *p*4*gm* in this example), the phases across the mirror line are opposite. An example of the latter is the pair 1 2 0 and 1 −2 0 with strong structure factors 2.8 and −2.8 V, respectively. It is clear that the relative strengths of coupling terms must be considered when selecting beams for comparison and that patterns with the above characteristics should be avoided when applying the expression (8).

7.2. $Bi_{12}GeO_{20}$

Expression (8) was applied to the example of levorotatory $Bi_{12}GeO_{20}$ used in Johnson & Preston (1994). Using the data of Svensson *et al.* (1979) for the laevorotatory enantiomorph gave the following calculated structure factors in Volts and degrees. v_c (0 4 0) = 1.9, V_L (25 −2 −1) = 0.17, 336, V_R (252 −1) = 0.17, 24. These give a value of −1.4 for $v_c \sin(\Phi_L - \Phi_R)$, in agreement with the experimental observation that I_R is greater than I_L.

8. Two-path cancellation

It is tempting to try the addition of related paths to see if a more stringent approach to cancellation can be obtained.

Choosing two paths in the scattering diagram of Fig. 8 that are symmetrically disposed about the *k* axis, the indices for F of path 1 (dotted line) when those for *V* are (*h* −1 −1) and (*h* − 1, −2*k*, −1) and for F of path 2 (full line) are (*h* + 1, −2*k*, −1). Combining the terms in (9) for both these paths yields, after substituting the cos and sin terms used above for A and B and some trigonometric manipulation, the influence of each atom at *x y z* in (9) to be

$$16\cos(2\pi x)\sin(2\pi hx)\cos(2\pi hx)\{\cos(2\pi ky)\cos(2\pi lz) - \sin(2\pi ky)\sin(2\pi lz)\}.$$

It is not clear to the author how this expression leads to any conclusion about cancellation that is superior to that already advanced.

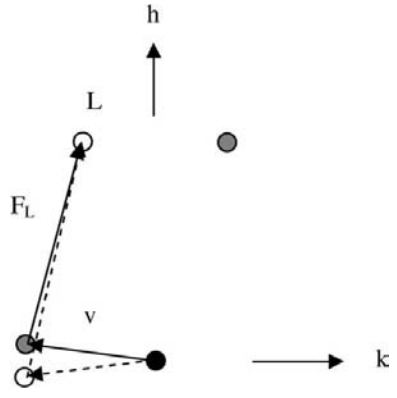

Figure 8
Definition of two paths to L symmetrically disposed about the *k* axis.

The above expression is for *P*222 with plane group symmetry *p*2*mm*. Extension to more complex ZOLZ symmetries is made by invoking the general relationships between structure factors for the plane groups when making substitutions into (8). These relationships are given in Table 1.4.3.A of the *International Tables for Crystallography* (1993).

9. Application to trigonal point groups

The case when no mirror lines are present, point group 3, presents the serious experimental difficulty of alignment for small tilts. Experimental tests at a threefold axis ($Bi_{12}GeO_{20}$ ⟨111⟩ (see Johnson & Preston, 1994) showed the only clearly recognizable alignment was the exact zone-axis pattern. The hand is then best determined by comparison of the ZOLZ pattern to that of a multislice calculation.[11] This situation also applies in the case of point groups 4 and 6.

For the remaining two threefold point groups, 321 and 312, (6) does not apply, as the equality of the amplitudes of the pair of FOLZ reflections which break the ZOLZ mirror line, used in its derivation, is no longer true. The equation could be used if the experimental difficulty of accurately tilting at right angles to one of the three polar twofold axes can be surmounted and the phase of the ZOLZ coupling term, v_c, which is now complex, could be taken into account. In this instance the modification to (6) is to the argument of the sin term, which is now $(\Phi_L - \Phi_R + \omega_c)$, where ω_c is the phase angle of v_c defined in the direction L to R.

In dealing with the threefold point groups it is wise to recognize that confusion can easily arise when defining axes and settings. The paper by Donnay & Le Page (1978) summarizes the situation for the low quartz structure where literature comparisons are complicated by a multitude of approaches.

Two further, more general recommendations are worth stating. Great care must clearly be taken in definitions at all steps in the process of interpreting the CBED pattern. The paper by Saxton *et al.* (1983) on sign conventions in electron diffraction and imaging is useful here. In addition, a physical property, such as optical rotation, should be associated with the crystal used in a chiral-determining experiment. Without this additional step there is no way other investigations may check the result. Making this association was suggested by Glazer & Stadnicka (1989) in their paper on structure–property relationships and terminology in the non-centrosymmetric crystal classes.

10. Application to zone-axis patterns

When the Cowley & Moodie expansion is applied to a zone-axis pattern, it is possible to derive a general expression similar to that found above for the tilted case. However, it is more complex, especially in the case of a minor zone, where the close neighbourhood of the FOLZ requires the inclusion

[11] It would be prudent to test the software used against experimental results taken from a crystal of known hand before accepting a result.

of inter-zone paths. The complexity is due to the presence of many beams of similar weight making the resulting expressions unwieldy.

11. Conclusion

It is apparent that patterns taken for the purpose of hand determination, when recorded at tilts of a few or more degrees away from a major zone axis, are more readily analyzed than the zone-axis patterns. Further, the experiment is facilitated since the major zone axes are more easily recognized and indexed than the minor zone axes, and alignment is particularly straightforward when a ZOLZ mirror line is present. These factors are especially important when dealing with large unit cells. A further advantage of the tilted experiment is that the tilt may be varied to detect various pairs of sensitive reflections and the measurement easily repeated. This again is of particular advantage when dealing with a complicated structure.

Subsequent to the paper of Johnson & Preston (1994), where a single pattern is used for the identification of hand, Inui *et al.* (2003) published a paper on the determination of chirality by CBED, again with single patterns but using those taken at a minor zone axis. They included a useful table of indices of equivalent reflections and the appropriate zone axes for their observation. They emphasize the use of Bijvoet pairs, which are any two symmetry equivalents which differ only by phase and have been referred to in this paper as equivalent pairs. The difference between the experimental technique used by Johnson & Preston and that of Inui *et al.* is that the former use a ZOLZ intensity mirror to enable orientation and the latter use a geometric mirror line that bisects Bijvoet pairs. These geometric lines are symmetry lines $m - m'$ in their paper. They would be mirror lines of intensity under conditions of pure kinematic scattering. Thus they are not the projected mirror lines of symmetry referred to in this paper. The lack of intensity symmetry makes the correct orientation difficult to recognize.

There are some aspects of the paper by Inui *et al.* (2003), which require comment. It is claimed that 'chiral identification can be made easily by inspecting the asymmetric intensity distribution of the Bijvoet pairs of reflections . . . '. Amplitude–phase diagrams are then used to determine the relative intensities between specific equivalent reflections (Bijvoet pairs), and thus the hand. It is not clear how their amplitude–phase diagrams take account of the many paths of comparable weight to a reflection *via* other beams in the pattern. Only amplitude–phase diagrams for two of many possible two-vector paths are shown. It is readily seen from the Cowley and Moodie series expansion that such an approach may lead to false conclusions as it does not give appropriate weights to first- and second-order scattering paths and, importantly, omits consideration of the many other contributions to the amplitude of a reflection *via* other paths. This latter omission is particularly important for the case of a minor zone-axis orientation, where there are a variety of multiple scattering paths of similar influence. In the case of a large unit-cell structure, at a minor zone axis there will be an even closer coupling between zones and many beams present. It is essential to understand their effect.

All the examples given by Inui *et al.* (2003) are taken at minor zone axes. This increases the proximity of the FOLZ to the ZOLZ and hence the coupling between them. This coupling should be taken into account, even though the interpretation requires only a comparison of the intensity distribution in one Laue zone to distinguish the hand.[12] At least a second-order coupling between the zones is required in any type of calculation to make this comparison correctly. Although not specifically stated, their calculated patterns must be of multiple beam type to accomplish this. Comparison of these with experiment will determine the hand, as shown for Te for example. Phase–amplitude diagrams are then unnecessary. The apparent lack of second-order coupling between zones in their phase–amplitude approach is confusing. As demonstrated in the present paper, it is important to consider the relative weights of *all* the various multiple scattering paths to a reflection in determining its intensity.

The fewer multiple scattering paths present in tilted patterns, when compared with those in a zone-axis pattern, simplify the application of the Cowley and Moodie series expansion and lead to simple formulae which require the knowledge of only a few structure factors and their phases to determine the enantiomorph from the sign of the intensity difference between a pair of equivalent reflections. However, it is clear from the formulae obtained that care should be taken so all paths of significant weight to these reflections are considered. It has been shown that an approximate cancellation of those two segment paths that do not involve the coupling vector between the equivalent reflections occurs in the case of tilted patterns when a mirror line is present in the zero Laue zone. In the case of zone-axis patterns, many paths of similar weight would need to be considered before a simple solution to the problem can be obtained.

It is a pleasure to acknowledge the helpful comments and suggestions made by Professor A. F. Moodie, Dr P. N. H. Nakashima and Dr M. Saunders. In particular thanks is due to Mr D. M. Jones for his interest and for many useful discussions.

References

Cowley, J. M. & Moodie, A. F. (1962). *J. Phys. Soc. Jpn*, **17**, Supp B-II, 86–91.
Donnay, J. D. H. & Le Page, Y. (1978). *Acta Cryst.* A**34**, 584–594.
Glazer, A. M. & Stadnicka, K. (1989). *Acta Cryst.* A**45**, 234–238.
Gjønnes, J. & Moodie, A. F. (1965). *Acta Cryst.* **19**, 65–67.
Goodman, P. & Johnson, A. W. S. (1977). *Acta Cryst.* A**33**, 997–1001.
Goodman, P. & Secomb, T. W. (1977). *Acta Cryst.* A**33**, 126–133.
Inui, H., Fujii, A., Tanaka, K., Sakamoto, H. & Ishizuka, K. (2003). *Acta Cryst.* B**59**, 802–810.

[12] This assumes that the index has been correctly assigned using at least two zones (Spence *et al.*, 1994).

Johnson, A. W. S. & Preston, A. R. (1994). *Ultramicroscopy*, **55**, 348–355.
Moodie, A. F. (1972). *Z. Naturforsch. A*, **27**, 437–440.
Saxton, W. O., O'Keefe, M. A., Cockayne, D. J. H. & Williams, M., (1983). *Ultramicroscopy*, **12**, 75–79.
Smolin, Y. I. (1970). *Sov. Phys. Cryst.* **15**, 36.
Spence, J. C. H., Zuo, J. M., O'Keeffe, M., Marthinsen, K. & Hoier, R. (1994). *Acta Cryst.* A**50**, 647–650.
Svensson, C., Abrahams, S. C. & Bernstein, J. L. (1979). *Acta Cryst.* B**35**, 2687–2690.
Tanaka, M., Takayoshi, H., Ishida, M. & Endoh, Y. (1985). *J. Phys. Soc. Jpn*, **54**, 2970–2974.